Effect of deuteron temperature on iron forbidden-line intensities in rf-heated tokamak plasmas

K. Sato,* S. Suckewer, and A. Wouters
Plasma Physics Laboratory, Princeton University, P.O. Box 451, Princeton, New Jersey 08544-0451
(Received 8 May 1987)

Two line ratios, the forbidden line at 845.5 Å ($2s^22p\ ^2P_{1/2}-2s^22p\ ^2P_{3/2}$) to the allowed line at 135.7 Å ($2s^22p\ ^2P_{1/2}-2s2p^2\ ^2D_{3/2}$) in Fe XXII and the forbidden line at 592.1 Å ($2s^22p^4\ ^3P_2-2s^22p^4\ ^1D_2$) to the forbidden line at 1118.2 Å ($2s^22p^4\ ^3P_2-2s^22p^4\ ^3P_1$) in Fe XIX, have been measured as ion-temperature-sensitive line ratios during rf heating in the Princeton Large Torus. The results indicate that deuteron collisions in plasmas of high deuteron temperature have a noticeable effect on the intensity of the forbidden lines. Measured relative intensities are compared with values from level-population calculations, which include deuteron collisional excitation between the levels of the ground configuration. The agreement between the observed and calculated ratios is within 30%. A method for deuteron (or proton) temperature measurement in tokamak plasmas is discussed.

I. INTRODUCTION

A number of forbidden lines arising from magnetic dipole transitions of highly ionized ions have been identified in tokamak discharges.[1] In terms of fundamental atomic physics, these forbidden transitions enable the determination of the energy level structure in highly ionized ions. Forbidden lines are also useful in plasma diagnostic applications because their relatively long wavelengths facilitate Doppler broadening and shift measurements for ion temperature and plasma rotation.[2–5]

Intensity measurements of the forbidden lines of highly ionized ions are also of interest. In the Poloidal Divertor Experiment (PDX) tokamak, the titanium density in the central part of the plasma was determined from the absolute intensity measurement of the Ti XVII forbidden line at 3834 Å.[6] Measurements of the spatial distribution of forbidden line intensities were used to study ion transport during neutral beam injection on the Princeton Large Torus (PLT).[7] Relative intensity measurements of various line pairs resulting from magnetic-dipole transitions have provided new branching line pairs for spectral sensitivity calibration of spectrometers.[8] For theoretical purposes, Bhatia, Feldman, and others have calculated level populations in the ground-state configuration for the major metallic constituents of a tokamak (iron, nickel, chromium, titanium, and other elements).[9–14] Feldman and Doschek proposed the method of using ratios of highly ionized lines from optically allowed and forbidden transitions for electron density measurements.[15,16]

In connection with intensity measurements, we discuss the effect of heavy-particle (proton and deuteron) collisions on the intensity of forbidden lines of highly ionized ions. This effect can be applied for ion-temperature measurements in tokamak plasmas from intensity ratios of forbidden to allowed[17] or forbidden to forbidden lines. Except for the excitation of plasma impurity ions by charge-exchange recombination with energetic neutral beam hydrogen,[18–21] inelastic collisions between heavy particles are not generally considered to be significant excitation processes in plasma, because of the relatively low velocity of the impacting particle. In astrophysics, however, large proton-induced excitation rates between closely spaced hydrogen levels ($2s$-$2p$) in the solar chromosphere are evidence of the significance of heavy-particle excitation.[22] In high temperature laboratory plasmas, a similar situation is expected to occur in the closely spaced levels of the ground-state configuration of highly ionized ions.

The importance of proton collisions on the state populations for the $2s^22p^k$ configurations was discussed by Feldman *et al.*[9–16] They showed that the metastable level populations in ground-state configurations depend on the balance of the radiative decay rate and the collisional excitation rates of electrons and protons in plasmas with electron densities lower than several 10^{13} cm^{-3}, which is in the typical operating range of tokamaks.

Quantitative measurements of forbidden and resonance line intensities were made on PLT.[23] Comparison of the observed intensities with the calculated intensities indicated that the influence of proton collisions on the forbidden line intensity was uncertain in Ohmic-heated discharges. Relative intensities of $2s^22p^k$-$2s2p^{k+1}$ transitions in metallic ions were also measured,[24] and there were indications that for the C I–like ions, calculations which include proton-collisional excitation and deexcitation between the levels of the ground configuration are in better agreement with the measurements than calculations that do not include the influence of proton collisions.

In Ohmic-heated discharges with moderate electron densities (below 10^{14} cm^{-3}), the ion temperature is roughly half the 1–2-keV electron temperature. In this case, proton collision excitation has a small effect on the populating mechanism compared with the cascading

processes from $2s2p^{k+1}$ levels. However, proton excitation might become quite significant during additional heating. The intensity ratio of a forbidden line to an allowed line of Fe XVIII was measured during rf heating on the Institute of Plasma Physics JIPP-T-II-U tokamak at Nagoya.[17] The results at an electron density of 2×10^{13} cm^{-3} indicated that proton collisions had a noticeable effect on the intensity of the forbidden line at the time of heating.

In this paper, we present the measurement of forbidden line intensities during the ion-cyclotron-range-of-frequency (ICRF) heating in PLT deuterium discharges for the three lines:

Fe XXII 845.5±0.1 Å ($2s^2 2p\ ^2P_{1/2}$-$^2P_{3/2}$),

Fe XIX 1118.2±0.1 Å ($2s^2 2p^4\ ^3P_2$-$^3P_1$),

and

592.1±0.1 Å ($2s^2 2p^4\ ^3P_2$-$^1D_2$).

Time evolutions of the intensity ratios of forbidden to allowed transitions in Fe XXII and forbidden to forbidden transitions in Fe XIX are presented and compared with the calculated intensity ratios. [Partial energy and diagrams for Fe XIX and Fe XXII are shown in Figs. 1(a) and 1(b).]

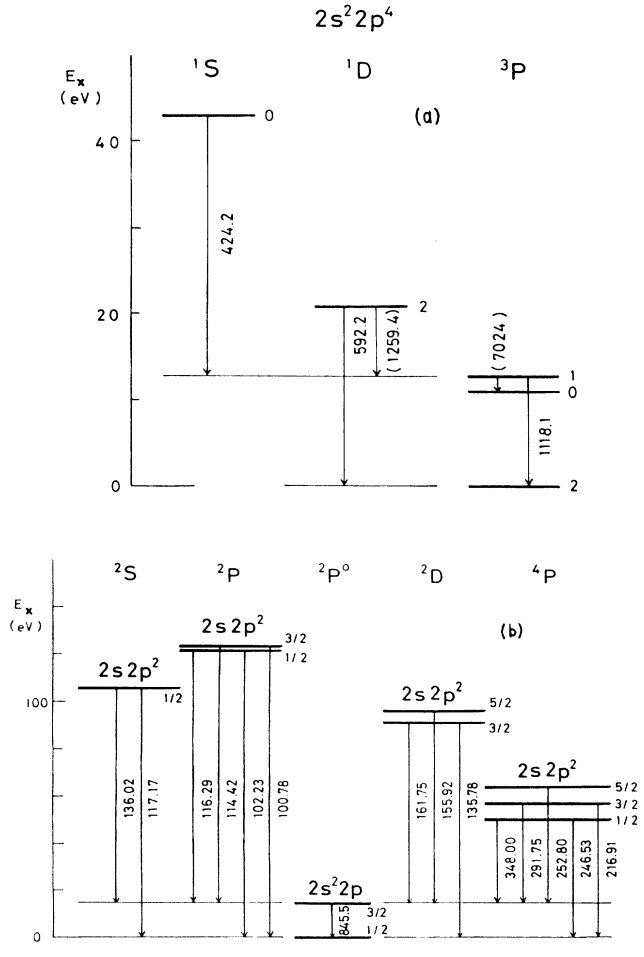

FIG. 1. Partial energy diagrams for (a) Fe XIX ion ground-state configuration and for (b) Fe XXII ion.

In the intensity ratio of the forbidden to allowed line, only the forbidden transition is sensitive to a deuteron temperature. The ratio is thus expected to be deuteron temperature dependent. Also, in the case of the ratio of the forbidden to forbidden line, the ratio might depend on the deuteron temperature because of the different dependence of the excitation rate of each transition on deuteron energy.

II. INSTRUMENTATION

Intensity measurements of the time evolution of iron forbidden lines were performed with a modified McPherson 1-m normal-incidence spectrometer. This instrument is equipped with two interchangeable gratings (1200-groves/mm Os grating blazed for 450 Å and 1200-grooves/mm MgF_2 overcoated aluminum grating blazed for 1500 Å), and multichannel detector (with a funneled CuI microchannel plate, with a P-20 phosphor screen connected by an 18-mm diameter fiber-optics extension to a cooled 1024 element photodiode array). The spectral range is from 250 to 2000 Å and the simultaneous coverage of wavelength is about 150 Å, resolution FWHM (with 50-μm entrance slit) is 0.7 Å in first order. Integration time is set to be 50 ms in normal usage.

This normal incidence multichannel spectrometer is highly efficient in detecting the spectral lines with wavelengths longer than 400 Å. For example, forbidden lines at 1354.1±0.1 Å in Fe XXI and 1079.4±0.1 Å in Fe XXIII (which are usually difficult to detect with a grazing incidence spectrometer[23]) have been observed as lines with strong intensity. Figures 2(a) and 2(b) show typical observed spectra in the 700–900 and 1100–1200 Å regions, which were of interest for the present work. In the measurement of the ratio of forbidden to forbidden transitions in Fe XIX, both lines 1118 Å and second order of 592 Å fall in the simultaneous coverage of the multichannel detector. This offers practical convenience in the measurements. To observe the 135-Å line of Fe XXII, two grazing incidence spectrometers were used: one is the soft x-ray multichannel spectrometer[25] "SOXMOS" and the other the grazing-incidence duochromator "GISMO."

Relative spectral sensitivity calibration of the normal incidence spectrometer was carried out by measuring two branching line pairs: (Cr XIX 979 Å/731 Å, Fe XXI 786 Å/585 Å).[8] In the measurement of the ratio of the 592-Å line to the 1118-Å line, relative sensitivities at these two points were extrapolated from the above-calibrated sensitivities. In measuring the intensity of the Fe XXII line at 845 Å relative to that at 135 Å, relative sensitivity at these two wavelengths in different spectrometers has been determined as follows: First, a branching line pair of the O VI line at 129 Å ($1s^2 2p$-$1s^2 4d$) and 498 Å ($1s^2 3p$-$1s^2 4d$) was measured simultaneously by two spectrometers. This provides a measure of the relative sensitivity of spectrometers. By extrapolating the calibrated points in the normal-incidence spec-

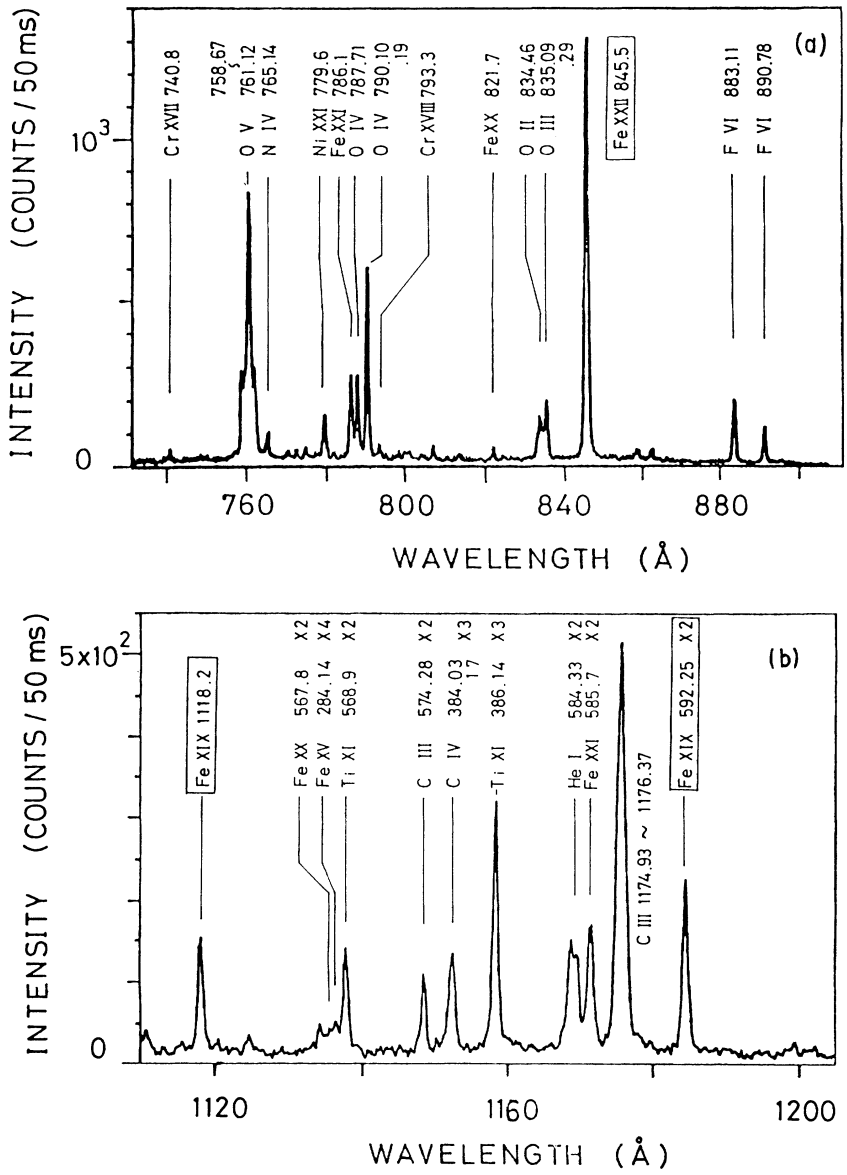

FIG. 2. Normal-incidence spectrum taken with MgF_2-overcoated aluminum grating during ICRF heating of a PLT plasma (a) in the 700 to 900 Å region and (b) in the 1100 to 1200 Å region.

trometer, the relative sensitivities at 135 and 845 Å were estimated. The error may be as large as 50% in this case. In addition to the weakness of the intensity of the O VI line pair, which originates from a highly excited state, this line pair is blended with other lines, the Ti XIV line at 129.4 Å and the Si XII line at 499.4 Å. But this should not prevent its use for sensitivity calibration in the case of a discharge with a relatively high concentration of oxygen impurities.

Sensitivity also depends upon the position where a spectral line falls on the coverage of a multichannel detector. In this connection, the intensity ratios of doublet lines in sodium-like ions Ti XII, Cr XIV, and Fe XVI (at 479.8 Å:460.7 Å, 411.9Å:389.8 Å, and 360.7 Å:335.4 Å, respectively) were measured by changing the position where the spectral line falls on the microchannel plate. This difference in the sensitivity of the multichannel detector has been included in analyzing the observed intensity ratios.

III. CALCULATIONS OF LEVEL POPULATIONS AND INTENSITY RATIOS WITH EMPHASIS ON HEAVY-PARTICLE IMPACT EXCITATION

In this section we present calculations of the effect of heavy-particle collisions on the populations of the transitions leading to the emission of Fe XXII lines at 845 and 135 Å, Fe XIX lines at 592 and 1118 Å, and the expected intensity ratios of these lines. Because of a short relaxation time of excited levels relative to ground level (also

relative to the tokamak's plasma time evolution), excited-level populations in the level n may be described by quasi-steady-state $dN_n/dt=0$. In other words, population may be written with the plasma parameters (electron density, temperature, etc.) and the population density at ground level. Here we concentrate on the case of an iron ion in ionization balance when the population of excited states (especially for low-lying levels) is practically unaffected by the density of ions in higher ionized states. In this case, excited level populations are given by a set of steady-state rate equations in the form

$$dN_n/dt=0=-N_n\left[\sum_{n\ (\neq m)}(A_{nm}+N_eS_{nm}+N_hS^h_{nm})\right]+\sum_{m\ (\neq n)}N_m(A_{mn}+N_eS_{mn}+N_hS^h_{mn}),\quad n\neq 1 \qquad (1)$$

($n=1$ corresponds to ground level). Here A_{nm} is the spontaneous transition probability from level n to m ($A_{nm}=0$ when $m>n$), S_{mn} is the electron-impact excitation rate coefficient if $m<n$ or deexcitation rate coefficient if $m>n$, N_h is the density of a heavy-particle ion (proton or deuteron), and the superscript h indicates a heavy particle collision. Coefficients A_{nm} for optically allowed transitions were taken from Fuhr *et al.*[26] The decay rates for the magnetic dipole transitions are given by Chen *et al.*[27] The electron-collisional rate coefficient was calculated from the collision strengths in the distorted wave approximation given by Mann[28] and Mason *et al.*[29,30] assuming a Maxwellian distribution of electron energies. The proton and deuteron excitation rate coefficients were calculated from the approximation formula given by Kastner *et al.*[31,32] Details of heavy particle collision excitation are provided in the Appendix.

At the temperatures and densities of tokamak plasmas, excited level populations of $2s2p^{k+1}$ ($\Delta n=0$ allowed transition) are determined predominantly by electron impact excitation from the ground-state configuration $2s^22p^k$. The highly ionized ions in a tokamak plasma are usually localized at the radial position where the electron temperature is about the same as the ionization energy of the considered ion. Since the excitation energy of $2s2p^{k+1}$ levels from $2s^22p^k$ is small compared with the ionization energy (about one tenth), electron impact excitation rates to the $2s2p^{k+1}$ levels are practically independent of electron temperature. The level populations of $2s2p^k3l$ configurations are small compared with the ones of $2s2p^{k+1}$ because of larger excitation energies which lead to smaller electron excitation rates. These levels of $\Delta n=1$ transitions are weakly coupled with $2s2p^{k+1}$ and $2s^22p^k$ levels. The influence of these higher levels was then neglected in the present calculations.

The state populations for the $2s^22p^k$ configurations depend on the balance of the radiative decay rate, the cascading processes from the $2s2p^{k+1}$ levels, the collisional rates of electrons, and especially the collisional rates of protons and deuterons. The excitation energies among the ground-state configurations are so small that electron excitation rates are only weakly electron temperature dependent. However, proton and deuteron excitation rates for ground-state configurations indicate strong dependence on their temperature. In Fig. 3 there are several representative electron collisional excitation rate coefficients and one for deuteron for the $\Delta n=0$ levels from the ground level of Fe XXII. The results of the calculation of intensity ratios of the Fe XXII forbidden line at 845 Å to the allowed line at 135 Å, and of the Fe XIX forbidden line at 592 Å to the forbidden line at 1118 Å are shown in Figs. 4(a) and 4(b) as a function of the temperature and density.

The deuteron excitation rate into the $2s^22p\ ^2P_{3/2}$ level of Fe XXII increases by about a factor of 8 as the temperature is increased from 0.5 to 3 keV. This increase primarily affects the ratio at the density below 5×10^{13} cm^{-3}. Therefore, the intensity ratio can provide a deuteron temperature if the electron density and temperature are known from other measurements. At higher density, collisional deexcitation of the $2s^22p\ ^2P_{3/2}$ level becomes competitive with the magnetic dipole radiative decay and the population of this level comes close to the Boltzmann distribution. Hence, the intensity ratio of the forbidden to allowed line can be used as an electron density diagnostic. There is only a small change in the values of the ratio in this density-sensitive range when the temperature is varied. The same conclusions apply to the intensity ratio of the forbidden to forbidden line in Fe XIX. In this case, after the lower excited level $2s^22p^4\ ^3P_1$ comes close to the Boltzmann distribution at high density (above 10^{14} cm^{-3}), the population of the higher level $2s^22p^4\ ^1D_2$, which is the upper level of the 592-Å line, is still far from equilibrium and therefore affected by the deuteron excitation. Thus there remains

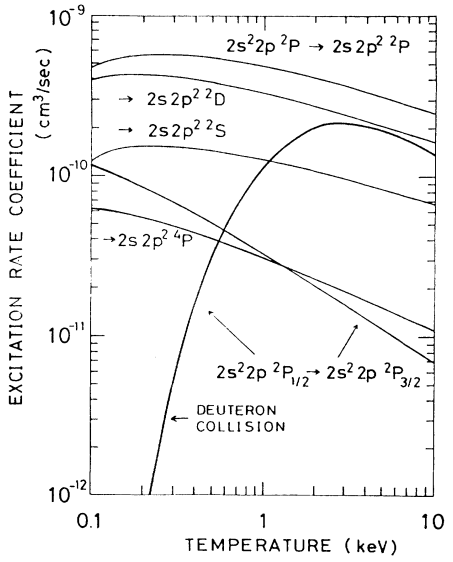

FIG. 3. Collisional excitation rate coefficients for the $\Delta n=0$ levels from the ground level of Fe XXII. Except for the forbidden transition between the ground-state configuration, electron impact excitation rates are calculated by summation over all possible J to J' transitions between individual levels of the LS term.

a significant change in the values of this ratio even in the high density range when the deuteron temperature is varied.

IV. EXPERIMENTAL RESULTS

The time evolutions of the two intensity ratios, the Fe XXII forbidden line at 845 Å relative to the allowed line at 135 Å and the Fe XIX forbidden line at 592 Å relative to the forbidden line at 1118 Å, were measured during ICRF heating. An rf heating was carried out in an ion minority fundamental ICRF heating regime. An rf at 30 MHz was applied to a deuterium plasma with $\sim 5\%$ ^{3}He minority at $B_t = 32$ kG. Since the intensity ratios depend also on electron density, heating with roughly constant density has been set as an experimental condition in order to clarify the influence of deuteron collisions on the forbidden line intensity.

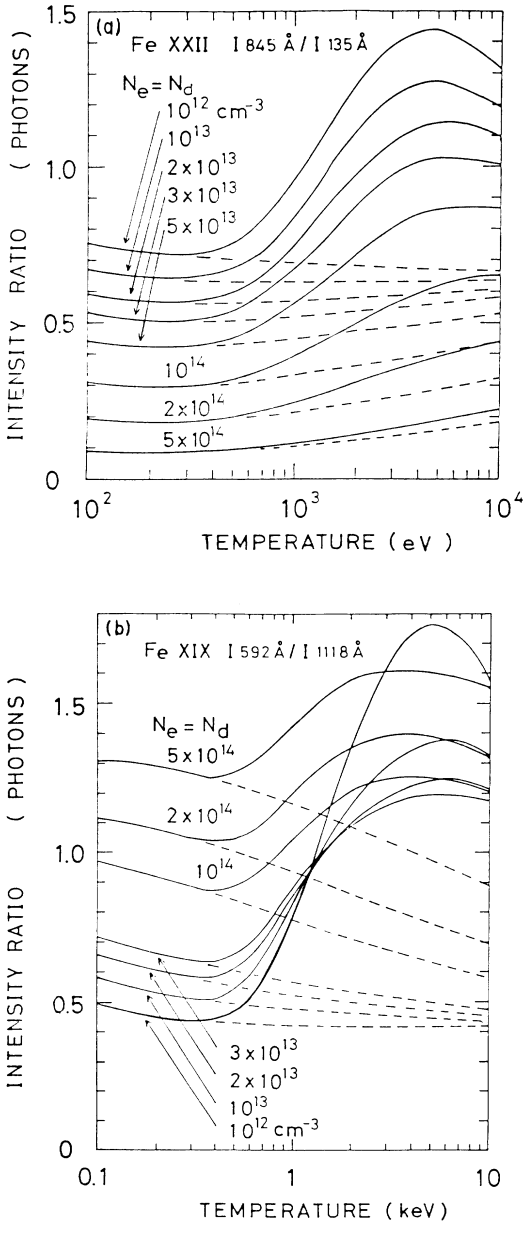

FIG. 4. (a) Intensity ratio of the indicated forbidden to allowed line in Fe XXII as a function of density and temperature. (b) Intensity ratio of the indicated forbidden to forbidden line in Fe XIX. In both cases, deuteron temperature and density are assumed to be the same as electron's. Dashed curves are calculated ratios without deuteron-ion collisions.

A. Fe XXII 845 Å/135 Å during 2.3 MW ICRF heating

An rf power of 2.3 MW was applied for 150 ms at $I_p = 460$ kA. The time evolutions of the 135-Å line were measured simultaneously with the multichannel spectrometer SOXMOS. Because of the problem of noise during the high-power ICRF heating, the intensity of the 135-Å line in the early period of the heating ($t = 400-550$ ms) was uncertain. Only the last period of the heating at 550–600 ms was available for reliable intensity ratio measurements.

Figure 5 shows the time evolution of the observed ratio of the 845-Å line to the 135-Å line and the line-averaged electron density during the heating. The central electron temperature obtained by electron-cyclotron-emission (ECE) measurements, and the ion temperature from a charge-exchanged fast neutral and neutron count rate are shown in the lower part of Fig. 5. The observed intensity ratio increases by about a factor of 2 during the heating. This increase may be attributed to the increased ion temperature, because of the constant

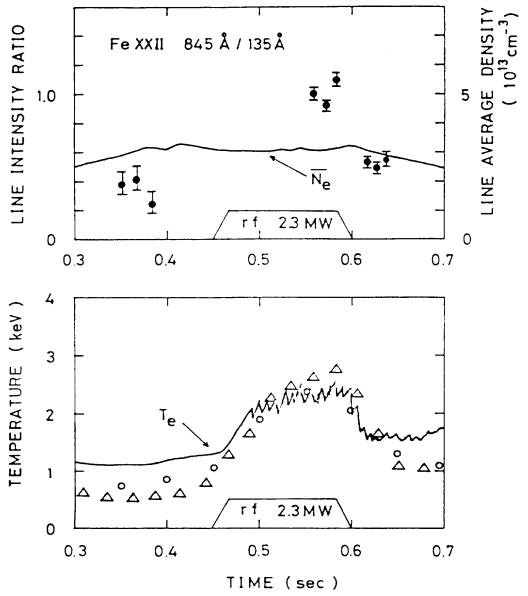

FIG. 5. Upper diagram: Time evolution of the indicated intensity ratio of the forbidden to allowed line of Fe XXII and line-averaged electron density. Lower diagram: ——, central electron temperature from ECE measurement. △, ion temperature from charge-exchanged fast neutral. ○, ion temperature from neutron count rate.

TABLE I. Measured and calculated intensity ratio of the 845.5-Å line to the 135.7-Å line in Fe XXII ion. (a) With rf power of 2.3 MW (450–600 ms). (b) With rf power of 1.3 MW (450–600 ms).

	Time (ms)	$\bar{n}_e$ (cm^{-3})	T_i (keV)	T_e (keV)	Line intensity ratio Calculation[a]	845.5/135.7-(Å) Measurement
			(a)			
ICRF heating with	350–400	3×10^{13}	0.6	1.1	0.45	0.4±0.1
constant electron	550–600	3×10^{13}	2.6	2.2	0.75	1.0±0.1
density	600–650	3×10^{13}	1.8	1.6	0.70	0.5±0.05
			(b)			
ICRF heating with	400	2.3×10^{13}	0.9	1.1	0.65	0.6±0.05
increased electron	550	3.2×10^{13}	1.6	1.4	0.70	0.8±0.05
density during rf	700	2.5×10^{13}	1.2	1.2	0.65	0.65±0.05

[a]Deuteron density was assumed $n_d=0.9n_e$ and central electron density n_{e0} was estimated to be 1.5 times the line-averaged density $\bar{n}_e$ in the calculation.

electron density and small effect of electron temperature on the ratio.

The comparison of the observed and calculated intensity ratios is given in Table I. Here the calculated ratio is derived from the measured electron density, electron temperature, and the ion (deuteron) temperature. The central electron temperature of 2.2 keV from the ECE measurement provides that the radial range where the Fe XXII ions (the ionization potential is 1.8 keV) exist is expected to be near the center of the plasma. Then, the central ion temperature is taken as the temperature which affects the intensity ratio in the calculation. As seen in the table, agreement of the observed ratio with the calculated one is 30% or better.

Note that the minority ion ICRF heating regimes provide an energetic ion "tail" production in minority,[33] but the intensity of Fe XXII at 845 Å should not be influenced by nonMaxwellian high-energy ion collisions (the excitation cross section for the 845-Å) line shows a decrease at higher than 3 keV incident energy). Also, relatively low concentration of minority ions gives only a small effect on the excitation rate for the 845-Å line.

B. Fe XXII 845 Å during 1.3 MW ICRF heating

About 450 ms after the start of the discharge, an rf power of 1.3 MW was applied for 150 ms at $I_p=600$ kA. The line-averaged electron density rises from 2.3×10^{13} cm^{-3} up to 3.2×10^{13} cm^{-3} in this case. The measurements of the 135-Å line intensity were performed with the grazing-incidence duochromator (GISMO). Here, the error caused from background levels and interfering lines (especially Fe XXIII strong line at 132.9 Å) was eliminated by subtracting the spectrometer off-line output at ±1.2 Å from the line center of 135 Å.

The intensity ratios observed before heating (350–400 ms), during heating (550–600 ms), and after heating (600–650 ms), and the comparison with the calculated ratios from the measured plasma parameters are listed in Table I. The central electron temperature of 1.4 keV from ECE measurements provides that the Fe XXII ions localize at the center of the plasma. The central ion temperature is then used to calculate the intensity ratio. In addition to the charge-exchanged fast neutral and neutron count rate for ion temperature measurement, the Doppler width line at 2665 Å of Fe XX (ionization potential is 1.58 keV) was measured to give a central ion temperature. The ion temperatures obtained from the above three different measurements agree well with each other.

Although the calculated ratio is expected to increase only 6% during the heating, the measured rate of increase in the observed ratio is fairly large (30%). This tendency towards a larger increasing rate in the ratio during the heating is similar to the previous results in IV A.

C. Fe XIX 592 Å/1118 Å during 400 kW ICRF heating

An rf power of 400 kW was applied to a relatively low density plasma ($\bar{n}_e=1.2\times10^{13}$ cm^{-3}) for about 180 ms at $I_p=500$ kA. The time evolutions of the 1118-Å line and the second order of the 592-Å line of Fe XIX were measured simultaneously with a multichannel normal in-

TABLE II. Measured and calculated intensity ratio of the 592.2- to the 1118.1-Å line in Fe XIX ion.

Time (ms)		$\bar{n}_e$ (cm^{-3})	T_i (keV)	T_e (keV)	Line intensity ratio Calculation[a]	592.2/1118.1-(Å) Measurement
450–500	before heating	1.2×10^{13}	0.9	1.5	0.8	0.9±0.1
550–600	during heating	1.2×10^{13}	1.5	1.7	1.0	1.2±0.1
600–650	during heating	1.2×10^{13}	1.6	1.7	1.0	1.0±0.2

[a]Deuteron density was assumed $n_d=0.9n_e$ and central electron density n_{e0} was estimated to be 1.5 times the line-averaged density $\bar{n}_e$ in the calculation.

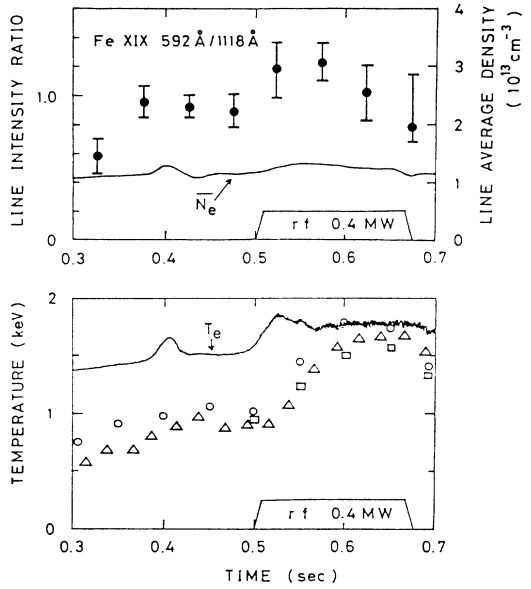

FIG. 6. Upper diagram: Time evolution of the intensity ratio of the indicated forbidden to forbidden line of Fe XIX and line-averaged electron density. Lower diagram: ——, central electron temperature from ECE measurement. △, ion temperature from charge-exchanged fast neutral. ○, ion temperature from neutron count rate. □, ion temperature from Doppler profile measurement for Fe XX 2665-Å line.

cidence spectrometer. The change of the plasma parameters and the observed ratio during the heating are shown in Fig. 6. As seen in the figure, electron density was kept constant.

Because of the high central electron temperature of 1.7 keV during the heating, Fe XIX (ionization potential is 1.46 keV) ions are expected to be located outside the plasma center. This can be seen also from the smaller values of the ion temperature from the Doppler width of the Fe XX line than from the charge-exchanged fast neutral and neutron count rate. Thus the ion temperature from the Fe XX 2665-Å line was used to calculate the ratio in Fe XIX. The comparison of the observed and calculated intensity ratio is given in Table II. Agreement of the observed ratio with the calculated one is better than 30%.

V. CONCLUDING REMARKS

The influence of heavy particle collisions on the forbidden line intensities of Fe XXII and Fe XIX has been demonstrated in PLT deuterium discharges during ICRF heating. Significant enhancement of forbidden-line emissions owing to the deuteron impact excitation during the heating is observed on the line intensity ratios in which one of the lines is due to a forbidden transition within the ground configuration and the other line is due to an allowed transition or another forbidden transition. The agreement between the measured and calculated ratios which include deuteron collisions excitation is quite good (about 30%). Thus such ratios in highly ionized iron ions may be used with some confidence for deuteron or proton temperature measurement. Investigation of a larger number of such ratios for various ions of different elements should reveal pairs of ions sensitive to deuteron (proton) temperature, which would, therefore, be suitable for such temperature measurements in different plasma conditions (different n_e, T_e).

The accuracy of relative sensitivity calibration is limited to 50% in this experiment. The comparison of the observed rates of increase in the ratio with those of calculation provides an additional aspect of the effect of deuteron collision, eliminating the uncertainty in sensitivity calibration. In this case, we found some systematic discrepancies between the experiment and theory: a larger increasing rate in the observed ratio during the heating than theoretically expected. This probably suggests that the deuteron excitation rate depends more strongly on the temperature. In the calculation of the intensity ratios, deuteron density was assumed to be 90% of the electron density, but a concentration of impurity ions may seriously affect the plasma composition (deuteron/electron). However, this should not contribute significantly to the ratio of line intensities and would rather have an effect in the opposite direction.

The approximation formula for heavy-particle collision excitation rates may be expected to give rates reliably within 50%. Also, the distorted-wave method for electron impact excitation appears to be accurate to within 30%.[34] Systematic quantitative investigations, both experimental and theoretical, will be required for further quantitative discussion. In the future, with increasing numbers of identified line pairs of ions for different elements and different stages of ionization, sensitive to proton and deuteron temperatures, it is expected that ratios of such line intensities will provide a method for quite accurate measurements of protons and deuteron temperatures in tokamak plasmas.

ACKNOWLEDGMENTS

The authors wish to thank our colleagues from the PLT and particularly J. Hosea and S. Bernabei for their support, P. Colestock, J. R. Wilson, J. Stevens, M. Ono, R. Kaita, and A. Cavallo for producing the discharge and providing us with information about ion temperature and electron temperature. We also would like to express our thanks to E. Hinnov for discussing PLT spectra, H. Fishman for his programming assistance, and L. Guttadora for his technical support. This work was supported by the U.S. Department of Energy under Contract No. DE-AC02-76CH03073.

APPENDIX

Explicit approximations for proton excitation cross sections and rate coefficients due to an electric quadrupole interaction are given by Kastner[31] and Kastner and Bhatia.[32] These approximations were obtained by dividing the range of proton energy into a low-energy region, in which semiclassical Coulomb excitation given by Alder *et al.*[35] is assumed, an intermediate-energy region in which a limiting expression due to Bahcall and Wolf[36] is

used, and a high-energy region, at which an excitation cross section shows E^{-1} dependence as noted by Bely and Faucher.[37] For the reader's convenience, the use of the related formulas for fine-structure transition among the ground-state configuration of iron is summarized here in order to make it easy to convert from proton excitation to deuteron excitation.

1. Low energy range

The excitation cross section is given by

$$Q_L=(Z_1e/\hbar V_i)^2a^{-2}(e^2a_0^4B_{E2})f_{E2}(\xi)\ , \tag{A1}$$

where V_i is the initial velocity in the center-of-mass system; Z_1 is charge of the incident particle; B_{E2} is the reduced radiative transition probability of electric quadrupole in unit of $e^2a_0^4$ ($=1.806\times10^{-52}$); and a and ξ are parameters defined by

$$\begin{aligned} a&=Z_1Z_2e^2/(m_0V_iV_f)\ ,\\ \xi&=(V_f^{-1}-V_i^{-1})Z_1Z_2e^2/\hbar\ , \end{aligned} \tag{A2}$$

with Z_2 being the charge of the target ion, and m_0 the reduced mass of the projectile and the target ion, V_f the final velocity in the center-of-mass system, and $f_{E2}(\xi)$ the classical orbital function for collisions in a Coulomb potential.

In the case of collisions between an iron ion and a proton or deuteron, the ratio of mass is large, so that the reduced mass is simply approximated as proton or deuteron mass. Also, velocity in a center-of-mass system is approximated as proton or deuteron velocity, because the thermal temperature of an iron ion as an impurity in the plasma is considered the same as the proton or deuteron temperature (due to the collisional relaxation).

By defining for a transition of given energy difference ΔE (in eV unit) the quantities $\chi=E_i/\Delta E$ (E_i: incident heavy-particle energy) and $K=\Delta E/Z_2^2$, the expression for Q_L of proton or deuteron collision may be rewritten in a simple form:

$$\begin{aligned} Q_L&=(2M/\hbar^2e^2)(1.60\times10^{-12}\ \text{K})(\chi-1)B_{E2}f_{E2}(\xi)\ \text{cm}^2\ ,\\ \xi&=(e^2M^{1/2}/\sqrt{2\hbar})(1.60\times10^{-12}\ \text{K})^{-1/2}\\ &\quad\times[(\chi-1)^{-1/2}-\chi^{-1/2}]\ , \end{aligned} \tag{A3}$$

where M is the mass of the projectile. A polynomial function which fits the values of $f_{E2}(\xi)$ tabulated by Alder *et al.* is

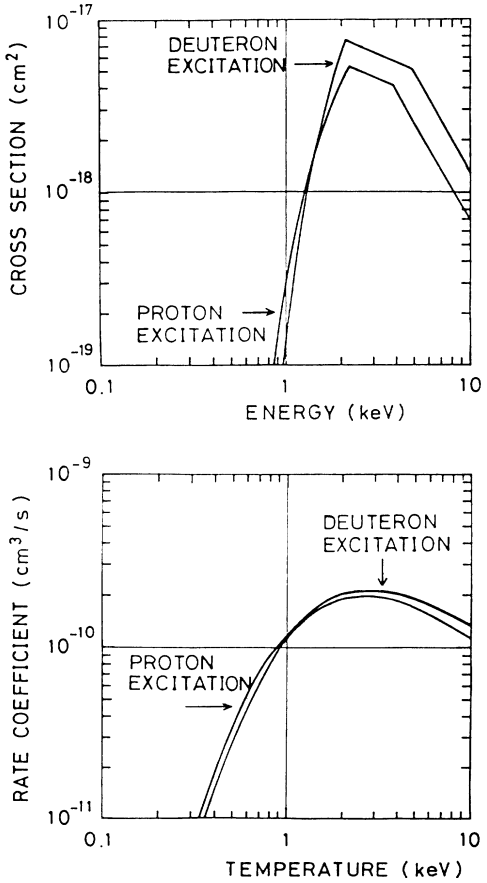

FIG. 7. Cross section and rate coefficient for proton and deuteron excitation of the transition Fe XXII ($2s^22p\ ^2P_{1/2}$-$^2P_{3/2}$).

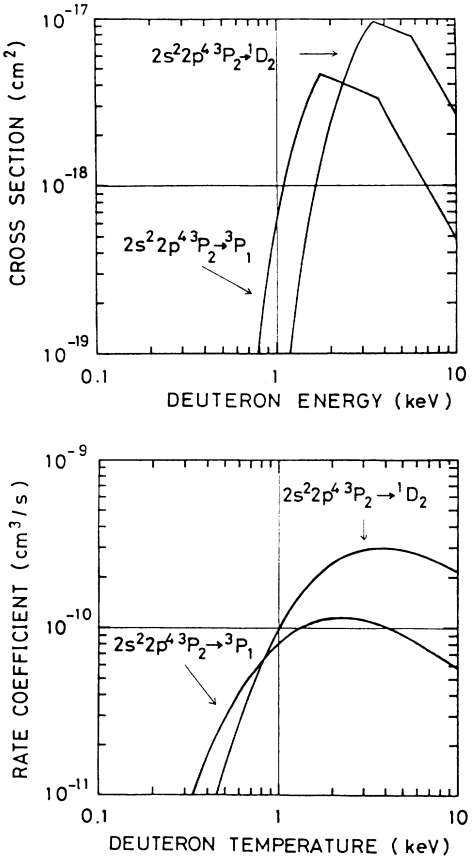

FIG. 8. Deuteron excitation cross section and rate coefficient for the transitions Fe XIX ($2s^22p^4\ ^3P_2$-$^3P_1$) and ($2s^22p^4\ ^3P_2$-$^1D_2$).

$$\log_{10} f_{E2}(\xi) = -0.046\,959 + 0.101\,04\xi - 3.310\,43\xi^2 + 2.7471\xi^3 - 1.3405\xi^4 + 0.337\,18\xi^5 - 0.032\,77\xi^6 \ . \quad \text{(A4)}$$

B_{E2} is related to the electric quadrupole transition probability A_q:

$$B_{E2} = (\hbar/8\pi)\{\lambda[(2\lambda+1)!!]^2/(\lambda+1)\} \times [c\hbar/(1.60\times10^{-12}\,\Delta E)]^{2\lambda+1} \times (e^2 a_0^4)^{-1} A_q (2J_f+1)/(2J_i+1) \ , \quad \text{(A5)}$$

where λ is the multipole order ($\lambda=2$ in the electric quadrupole case); J_f and J_i are the total angular quantum number of the upper level and the lower level, respectively.

2. Intermediate energy range

The cross section given by Bahcall and Wolf which holds for $\xi < 1$ is

$$Q_I = (\pi e^2 a_0^2/2\sqrt{2\hbar})[S_q(2J_f+1)/(2L_f+1)(2S_f+1)] \times [M/(1.60\times10^{-12}\,\Delta E)]^{1/2}\chi^{-1/2}\ \text{cm}^2 \ , \quad \text{(A6)}$$

where S_q is the radial quadrupole moment in unit of ea_0^2, and L_f, S_f, J_f are the LS quantum numbers of the final level. The value $\frac{1}{2}$ is a factor empirically found to give reasonable cross section for a number of different transitions. This expression (A6) is valid for $\chi > \chi_m$, where χ_m is found as an intersection value for which $Q_L(\chi_m) = Q_I(\chi_m)$.

3. High energy range

The cross section in the high energy range which holds for $\xi < 0.1$ is given by

$$Q_H = \frac{(\pi e^2 a_0^2 \sqrt{M}/2\sqrt{2\hbar})[S_q(2J_f+1)/(2L_f+1)(2S_f+1)][(10\xi/\chi^{1/2})+(1-10\xi)/\chi]}{(1.60\times10^{-12}\,\Delta E)^{1/2}}\ \text{cm}^2 \ . \quad \text{(A7)}$$

From the definition of ξ, for large χ, ξ may be approximated by

$$\xi = (e^2\sqrt{M}/2\sqrt{2\hbar})(1.60\times10^{-12}\ \text{K})^{-1/2}(\chi^{-3/2}+0.75\chi^{-5/2}), \quad \chi \gg 1 \ . \quad \text{(A8)}$$

At the transition value $\xi_t = 0.1$,

$$\chi = \chi_t \simeq (0.2\sqrt{2\hbar}/e^2\sqrt{M})^{-2/3}(1.60\times10^{-12}\ \text{K})^{-1/3} \ . \quad \text{(A9)}$$

Equation (A7) is therefore valid for $\chi \geqq \chi_t$.

Figure 7 represents the cross section and rate coefficient for proton and deuteron excitation of the transition Fe XXII ($^2P_{1/2}$-$^2P_{3/2}$) in the present approximation. Deuteron excitation cross section and rate coefficient for the transitions Fe XIX ($^3P_2$-$^3P_1$) and ($^3P_2$-$^1D_2$) are illustrated by Fig. 8.

The appropriate expression for cross section is summarized as follows: low energy range Q_L for $\chi \leqq \chi_m$, intermediate energy range Q_I for $\chi_m < \chi < \chi_t$, high energy range for $\chi \geqq \chi_t$. If $\chi_m > \chi_t$, the intersection value χ'_m is defined for which $Q_L(\chi'_m) = Q_H(\chi'_m)$: then the cross section is $Q_L(\chi \leqq \chi'_m)$ and $Q_H(\chi > \chi'_m)$.

The excitation rate coefficient is calculated by the average over a Maxwellian velocity distribution. Some analytical forms for the proton excitation rate are described in Refs. 31 and 32.

*Permanent address: Institute of Plasma Physics, Nagoya University, Chikusa-ku, Nagoya 464, Japan.

[1](Since a large number of papers on the indentification of forbidden transitions have been published, only a recent comprehensive paper is referenced.) V. Kaufman and J. Sugar, J. Phys. Chem. Ref. Data **15**, 321 (1986).
[2]S. Suckewer and E. Hinnov, Phys. Rev. Lett. **41**, 756 (1978).
[3]H. Eubank *et al.*, *Proceedings of the Seventh International Conference on Plasma Physics and Controlled Nuclear Fusion* (IAEA, Inssbruck, Austria, 1978).
[4]S. Suckewer and E. Hinnov, Bull. Am. Phys. Soc. **23**, 875 (1978).
[5]S. Suckewer, Phys. Scr. **23**, 72 (1981)
[6]S. Suckewer *et al.*, Nucl. Fusion **19**, 1681 (1979).
[7]S. Suckewer *et al.*, Nucl. Fusion **24**, 815 (1984).
[8]B. Denne and E. Hinnov, J. Opt. Soc. Am. B **1**, 699 (1984).
[9]U. Feldman, G. A. Doschek, C.-C. Cheng, and A. K. Bhatia, J. Appl. Phys. **51**, 190 (1980).
[10]A. K. Bhatia, U. Feldman, and G. A. Doschek, J. Appl. Phys. **51**, 1464 (1980).
[11]A. K. Bhatia, J. Appl. Phys. **53**, 59 (1982).
[12]A. K. Bhatia and U. Feldman, J. Appl. Phys. **53**, 4711 (1982).
[13]A. K. Bhatia, U. Feldman, and J. F. Seely, At. Data Nucl. Data Tables **35**, 319 (1986).
[14]A. K. Bhatia, U. Feldman, and J. F. Seely, At. Data Nucl. Data Tables **35**, 449 (1986).
[15]G. A. Doschek and U. Feldman, J. Appl. Phys. **47**, 3083 (1976).
[16]U. Feldman and G. A. Doschek, J. Opt. Soc. Am. **67**, 726 (1977).
[17]K. Sato *et al.*, Phys. Rev. Lett. **56**, 151 (1986).
[18]R. C. Isler and L. E. Murray, Appl. Phys. Lett. **42**, 355 (1983).
[19]S. Suckewer *et al.*, Appl. Phys. Lett. **45**, 236 (1984).

[20]R. J. Fonck, D. S. Darrow, and K. P. Jaehnig, Phys. Rev. A **29**, 3288 (1984).
[21]R. C. Isler, Nucl. Fusion **24**, 1599 (1984).
[22]E. M. Purcell, Astrophys. J. **116**, 457 (1952).
[23]S. Suckewer and E. Hinnov, Phys. Rev. A **20**, 578 (1979).
[24]B. C. Stratton, H. W. Moos, S. Suckewer, U. Feldman, J. F. Seely, and A. K. Bhatia, Phys. Rev. A **31**, 2534 (1985).
[25]A. W. Wouters, J. L. Schwob, S. Suckewer, F. P. Boody, R. Hulse, and J. Schivell, Rev. Sci. Instrum. **56**, 849 (1985).
[26]J. R. Fuhr, G. A. Martin, W. L. Wiese, and S. M. Younger, J. Phys. Chem. Ref. Data **10**, 305 (1981).
[27]K. T. Chen, Y. K. Kim, and J. P. Desclaux, At. Data Nucl. Data Tables **24**, 111 (1979).
[28]J. B. Mann, At. Data Nucl. Data Tables **29**, 407 (1983).
[29]H. E. Mason and P. J. Storey, Mon. Not. R. Astron. Soc. **191**, 631 (1980).
[30]M. Loulergue, H. E. Mason, H. Nussbaumer, and P. J. Storey, Astron. Astrophys. **150**, 246 (1985).
[31]S. O. Kastner, Astron. Phys. **54**, 255 (1977).
[32]S. O. Kastner and A. K. Bhatia, Astron. Astrophys. **71**, 211 (1979).
[33]J. Hosea *et al.*, Princeton Plasma Physics Laboratory Report No. PPPL-2117, 1984 (unpublished).
[34]D. H. Sampson, S. J. Goett, and R. E. H. Clark, At. Data Nucl. Data Tables **30**, 125 (1984).
[35]K. Adler, A. Bohr, T. Huus, B. Mottelson, and A. Winter, Rev. Mod. Phys. **28**, 432 (1956).
[36]J. B. Bahcall and R. A. Wolf, Astrophys. J. **152**, 701 (1968).
[37]O. Bely and P. Faucher, Astron. Astrophys. **6**, 88 (1970).